Optimization of Soft Magnetic Properties in $Fe_{82}Nb_2B_{14}RE_2$ (RE = Y, Gd, Tb and Dy) Group of Amorphous Alloys

A. Chrobak[a,*], G. Haneczok[b], O. Zivotsky[c], A. Hendrych[c], J. Kansy[b] and B. Kotur[d]

[a]University of Silesia, Institute of Physics, Uniwersytecka 4, 40-007 Katowice, Poland
[b]University of Silesia, Institute of Materials Science (SMCEBI), 75 Pułku Piechoty 1, 41-500 Chorzów, Poland
[c]VŠB-Technical University of Ostrava, Institute of Physics, 17. listopadu 15, 708 33 Ostrava-Poruba, Czech Republic
[d]Ivan Franko National University of Lviv, Kyryla and Mefodia St. 6, 79005 Lviv, Ukraine

Enhancement of soft magnetic properties in the selected group of amorphous alloys was examined by different experimental methods. It was shown that permeability for annealed samples (at T_a for 1 h; 300 K < T_a < 900 K) plotted vs. T_a shows a maximum at which is 700, 725, 725, and 750 K for $Fe_{82}Nb_2B_{14}Y_2$, $Fe_{82}Nb_2B_{14}Gd_2$, $Fe_{82}Nb_2B_{14}Tb_2$ and $Fe_{82}Nb_2B_{14}Dy_2$ alloy, respectively. For samples after the optimization annealing permeability is at least 10 times higher than in the as-quenched state. The optimized microstructure is free of iron nanograins and corresponds to so-called relaxed amorphous phase.

1. Introduction

It is well known that soft magnetic properties of iron based amorphous alloys can be enhanced by applying a specific annealing at temperatures close to crystallization temperature. After such annealing a low field magnetic permeability can increase even 20 times and a coercive field can go down below 1 A/m [1–8]. The observed effects are explained by formation of an optimized microstructure which in general can be of two types: (i) iron nanograins embedded into a residual amorphous phase [1–5] or (ii) the so-called relaxed amorphous phase free of iron nanograins for which free volume and internal stresses are significantly reduced [2, 6–8]. The type of the optimized microstructure strongly depends on alloying additions and parameters of the applied annealing. Influence of RE (rare earth) additions with a high localized magnetic moment on magnetic properties and crystallization of the same group of amorphous alloys in the as-quenched state have been already reported in [9] and [10], respectively. It was shown for example that 2 at.% of RE addition leads to an increase of the Curie temperature by no more than 34 K (for $Fe_{82}Nb_2B_{14}Gd_2$) in relation to the reference $Fe_{82}Nb_2B_{14}Y_2$ alloy (T_C = 416 K) [9]. A strong spin–orbit coupling of Tb and Dy atoms leads to an additional magnetic anisotropy of the examined alloys and to a magnetic hardening (permeability drops down about 5 times and a finger-print domain structure appears) [10]. Moreover, a localized magnetic moment of RE atoms cause an increase of the activation enthalpy of crystallization by about 0.8 eV (4.4 eV for the $Fe_{82}Nb_2B_{14}Y_2$ and 5.2 eV for the $Fe_{82}Nb_2B_{14}Tb_2$ alloy) [10].

The aim of the present paper is to study the optimization of soft magnetic properties in the family of amorphous alloys of type $Fe_{82}Nb_2B_{14}RE_2$ (RE = Y, Gd, Tb and Dy). The key point is to examine an influence of different thermal annealing on magnetic properties and formation of the so-called relaxed amorphous phase. The $Fe_{82}Nb_2B_{14}Y_2$ alloy with non-magnetic yttrium is taken as a reference alloy because Y has similar to RE atomic radius.

2. Experimental procedure and results

The examined amorphous alloys were prepared by applying a melt spinning technique in a helium atmosphere. The melt was prepared from pure binary $REFe_2$ (RE=Y, Gd, Tb, and Dy) and $NbFe_2$ compounds. The purity of the initial metals were : Fe (99.99 wt%), Y (99.96 wt%), Gd (99.96 wt%), Tb (99.96 wt%), and Dy (99.96 wt%). Rare earth metals in a form of binary compounds $REFe_2$ and $NbFe_2$ were primarily obtained by the arc-melting technique from metals of the same purity. The obtained alloys were in the form of strips with thickness and width of 20–25 μm and 3 mm, respectively. The melt spun ribbons in the as-quenched state were annealed at temperatures T_a (300 K < T_a < 900 K) for 1 h, and for annealed samples the following measurements were carried out: (i) low field magnetic permeability (Agilent meter E4980a, field 0.5 A/m), (ii) magnetization versus temperature (Faraday type magnetic balance, field 0.5 T, 300 K < T < 1100 K, heating rate 5 K/min) and (iii) Mössbauer spectra (standard transmission geometry with constant acceleration drive). Moreover, for selected samples, magnetic domain structure was examined using Zeiss optical microscope adopted for magneto-optical Kerr microscopy.

Figure 1 shows the low field magnetic permeability μ measured at room temperature for annealed samples

———
*corresponding author; e-mail: artur.chrobak@us.edu.pl
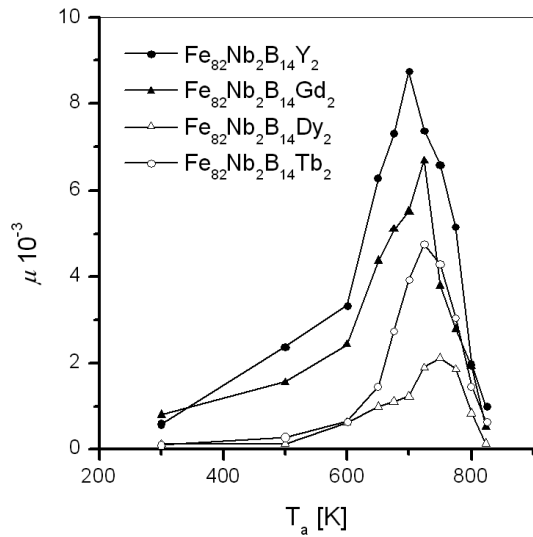
Fig. 1. Low field magnetic permeability measured at room temperature versus 1 h annealing temperature T_a.

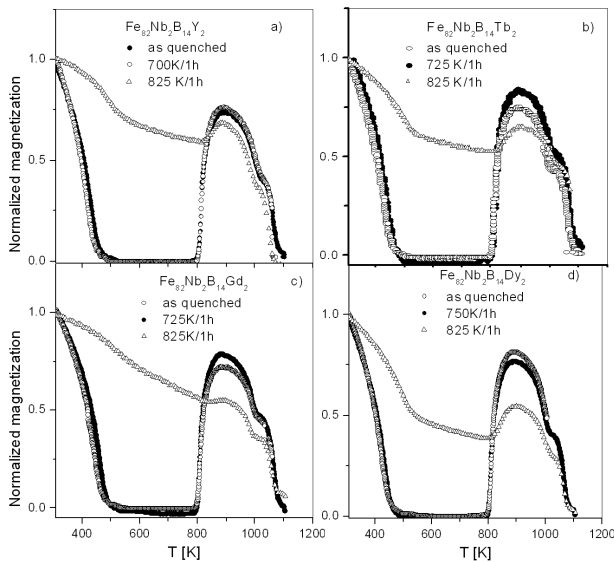
Fig. 2. Normalized magnetization versus temperature for sample preliminary annealed at different temperatures for (a) $Fe_{82}Nb_2B_{14}Y_2$, (b) $Fe_{82}Nb_2B_{14}Tb_2$, (c) $Fe_{82}Nb_2B_{14}Gd_2$, and (d) $Fe_{82}Nb_2B_{14}Dy_2$.

annealing at $T_a > T_{op}$. One can see that for samples in the as quenched states magnetization drops down with temperature and at $T > 450$ K the examined alloys are in paramagnetic state. In temperature range $800 \leq T \leq 900$ K magnetization in saturation strongly increases due to formation of iron nanograins which was confirmed by X-ray examinations and high resolution transmission electron microscopy observations [3]. At temperatures $T > 900$ K magnetization goes down up to the Curie temperature of the already formed crystalline phase. Similar curves were obtained for samples preliminary annealed for 1 h at T_{op} i.e. after the 1 h optimization annealing. In contrast, magnetization versus temperature for samples preliminary annealed at temperature $T_a = 850$ K (i.e. at $T_a \gg T_{op}$) do not show an intermediate paramagnetic state. This is obviously due to formation of iron grains (nanograins) during the preliminary annealing. In each examined case a residual amorphous phase with the Curie point at about 416–450 K and at higher temperatures some residual crystallization are detected. Figure 3a and b shows the Mössbauer spectra obtained for samples annealed for 1 h at temperature T_{op} and at $T_a > T_{op}$ of the $Fe_{82}Nb_2B_{14}Y_2$ and $Fe_{82}Nb_2B_{14}Tb_2$ alloy, respectively.
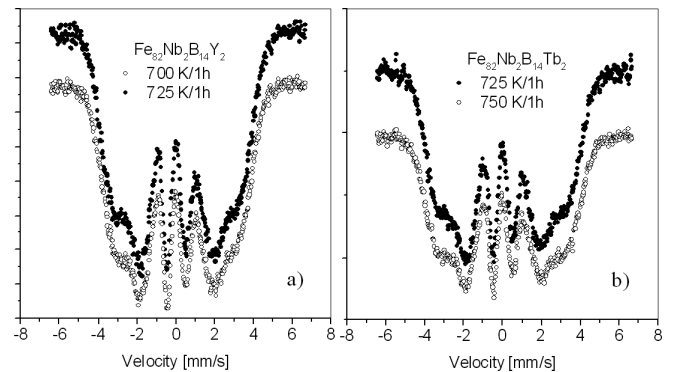
Fig. 3. Mössbauer spectra for the $Fe_{82}Nb_2B_{14}Y_2$ (a) and $Fe_{82}Nb_2B_{14}Tb_2$ (b) alloys, measured at room temperature for the samples annealed at temperatures T_{op} (the optimization and at higher temperature).
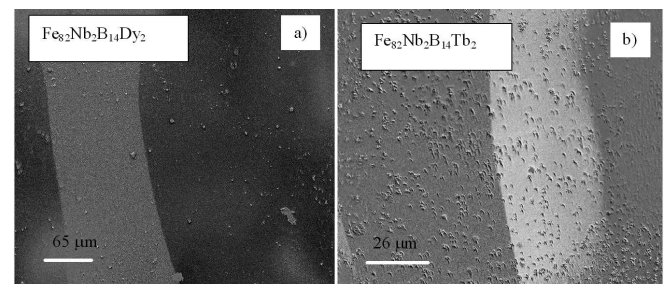
Fig. 4. Magnetic domain patterns obtained the Kerr microscopy observations for the $Fe_{82}Nb_2B_{14}Dy_2$ (a) and $Fe_{82}Nb_2B_{14}Tb_2$ (b) alloys annealed at $T_{op} = 750$ K and $T_{op} = 725$ K, respectively.

plotted versus T_a (for the as-quenched state $T_a = 300$ K). One can see that in all examined cases $\mu(T_a)$ curve shows a distinct maximum indicating that 1 h annealing at a well-defined temperature (denoted as T_{op}) causes a significant enhancement of the magnetic permeability. In fact, according to Fig. 1, annealing at T_{op} results in more than a tenfold increase of μ.

Figure 2 shows magnetization in saturation versus temperature determined for samples of different alloys in the as quenched states, after preliminary annealing at T_{op} (the optimization annealing) and after preliminary

One can see that the obtained spectra are typical for the amorphous phase rich in iron. Similar results are obtained for the $Fe_{82}Nb_2B_{14}Gd_2$ and $Fe_{82}Nb_2B_{14}Dy_2$ alloys. Figure 4a and b show magnetic domain patterns obtained by the Kerr microscopy for samples annealed at T_{op} for 1 h (the optimization annealing) for the $Fe_{82}Nb_2B_{14}Dy_2$ and $Fe_{82}Nb_2B_{14}Tb_2$ alloy, respectively. One can see that in both cases, the optimized microstructure corresponds to a well-developed large magnetic domains characteristic for a magnetic state free of internal stresses.

3. Discussion and conclusions

The results presented in Fig. 1 show that for all examined alloys magnetic permeability can be enhanced by applying 1 h annealing at temperatures T_{op}: 700, 725, 725, and 750 K for $Fe_{82}Nb_2B_{14}Y_2$, $Fe_{82}Nb_2B_{14}Gd_2$, $Fe_{82}Nb_2B_{14}Tb_2$ and $Fe_{82}Nb_2B_{14}Dy_2$ alloy, respectively. Figure 5 shows T_{op} and the optimized magnetic permeability (determined for samples after annealing at T_{op}) versus magnetic moment m of RE additions. One can see that in relation to a non-magnetic Y addition the temperature T_{op} slightly increases with increasing m. Similar effect was observed in [10] where it was shown that activation enthalpy of crystallization as well as crystallization heat depend on m in the same way. This means that high localized magnetic moment of RE atoms cause a slowing down of diffusion processes. Moreover, according to Figs. 1 and 5 the optimized magnetic permeability strongly decreases with increasing m which means that RE additions cause a hardening of the examined soft magnets — the highest effect is observed for alloys with Tb and Dy. This is understandable because Tb and Dy due to a strong spin–orbit coupling introduce to the system an additional magnetic anisotropy.
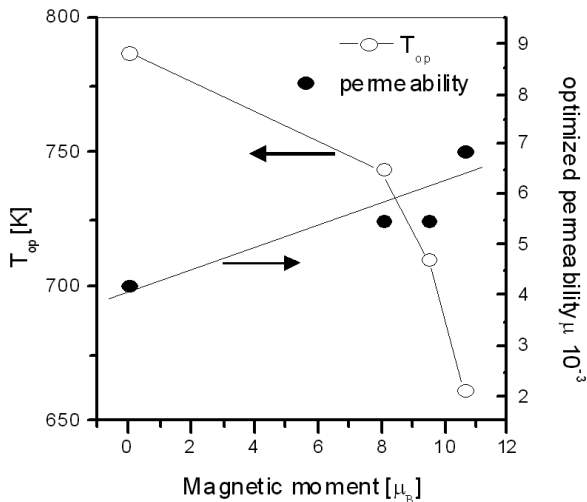

Fig. 5. Temperature T_{op} (1 h optimization annealing) and optimized magnetic permeability (determined for samples after 1 h optimization annealing) vs. magnetic moment of RE additions.

The results presented in Fig. 2a–d evidently show that nanocrystallization of iron in the examined alloys takes place at temperatures higher than 800 K. It is evident that for all alloys the preliminary 1 h annealing at 850 K leads to formation of a composite consisting of iron nanograins embedded into residual amorphous phase. In each case, the thermomagnetic curves do not show a paramagnetic region as it was observed for samples preliminary annealed at $T_a \leq T_{op}$ and furthermore, at higher temperatures a residual crystallization is observed. These two facts prove that the 1 h optimization annealing at T_{op} does not lead to the formation of iron nanograins. This conclusion is confirmed by the Mössbauer spectroscopy measurements. In fact, the spectra presented in Fig. 3a and b obtained for samples annealed at T_{op} and at temperature higher by 25 K are typical for an amorphous phase rich in iron. The most important is the fact that for all examined alloys spectra lines typical for iron nanograins (observed usually at velocity of about ± 6 mm/s) are not detected at all. Finally, taking into account the above arguments one can conclude that the optimized microstructure for the studied family of amorphous alloys is free of iron nanograins and corresponds to the relaxed amorphous phase. The magnetic domain structure, corresponding to the optimized microstructure, as shown in Fig. 4a and b, consists of regular large magnetic domains characteristic for a magnetic state free of internal stresses. The case of Tb and Dy due to a strong spin–orbit coupling is especially interesting. For these alloys the magnetic domain structure, corresponding to the as quenched state is of finger-print type [9] which means that in this case internal stresses play a dominant role. Comparing the results obtained in [9] (see Fig. 6 in [9]) and in the present paper one can conclude that the 1 h optimization annealing causes a drastic drop down of the internal stresses which manifests in a drastic change of the magnetic domain structure and an enhancement of the magnetic permeability.

The main conclusions of the present paper can be summarized as follows:

(i) The low field magnetic permeability of the examined alloys can be significantly enhanced (at least about 10 times) by applying a 1h annealing at temperatures T_{op} (700 K, 725 K, 725 K and 750 K for $Fe_{82}Nb_2B_{14}Y_2$, $Fe_{82}Nb_2B_{14}Gd_2$, $Fe_{82}Nb_2B_{14}Tb_2$ alloy and $Fe_{82}Nb_2B_{14}Dy_2$ alloy, respectively. (ii) In all examined cases the optimized microstructure corresponds to the so-called relaxed amorphous phase i.e. amorphous phase with significantly reduced free volume content as well as internal stresses. (iii) Magnetic domain structure corresponding to the optimized microstructure consists of relatively large regular domains indicating low level of internal stresses.

Acknowledgments

References

[1] M.E. McHenry, M.A. Willard, D.E. Laughin, *Prog. Mater. Sci.* **44**, 291 (1999).

[2] G. Haneczok, J. Rasek, *Def. Diff. Forum* **224-225**, 13 (2004).

[3] T. Kulik, *J. Non-Cryst. Solids* **287**, 145 (2001).

[4] J. Marcin, A. Wiedenmann, I. Skorvanek, *Physica B* **870**, 276 (2000).

[5] O. Zivotsky, K. Postava, L. Kraus, K. Hrabovska, A. Hendrych, J. Pistora, *J. Magn. Magn. Mater.* **322**, 1523 (2010).

[6] P. Kwapuliński, A. Chrobak, G. Haneczok, Z. Stokłosa, J. Rasek, J. Lelątko, *Mater. Sci. Eng. C* **23**, 71 (2003).

[7] Ł. Madej, G. Haneczok, A. Chrobak, P. Kwapuliński, Z. Stokłosa, J. Rasek, *J. Magn. Magn. Mater.* **320**, e774 (2008).

[8] A. Chrobak, G. Haneczok, D. Chrobak, Ł. Madej, G. Chełkowska, M. Kulpa, *J. Magn. Magn. Mater.* **320**, e770 (2008).

[9] A. Chrobak, V. Nosenko, G. Haneczok, L. Boichyshyn, B. Kotur, A. Bajorek, O. Zivotsky, A. Hendrych, *Mater. Chem. Phys.* **130**, 603 (2011).

[10] A. Chrobak, V. Nosenko, G. Haneczok, L. Boichyshyn, M. Karolus, B. Kotur, *J. Non-Cryst. Solids* **357**, 4 (2011).